Sustainable Waterborne Polylactide Coatings Enabled by Ionic Liquid Plasticization

Denys Baklan *, Victoria Vorobyova, Olena Sevastyanova *, Taras Karavaev, Oleksiy Myronyuk

Posted Date: 24 November 2025

doi: 10.20944/preprints202511.1672.v1

Keywords: polylactide; polymer; water dispersion coatings; polymer film; coating; glass transition temperature

 doi:10.20944/preprints202511.1672.v1

Article

Sustainable Waterborne Polylactide Coatings Enabled by Ionic Liquid Plasticization

Denys Baklan [1,*], Victoria Vorobyova [2], Olena Sevastyanova [3,*], Taras Karavaev [4] and Oleksiy Myronyuk [1]

[1] Department of Chemical Technology of Composite Materials, Chemical Technology Faculty, Igor Sikorsky Kyiv Polytechnic Institute, Beresteiskyi Ave. 37, 03056 Kyiv, Ukraine

[2] Physical Chemistry Department, Chemical Technology Faculty, Igor Sikorsky Kyiv Polytechnic Institute, Beresteiskyi Ave. 37, 03056 Kyiv, Ukraine

[3] Division of Wood Chemistry and Pulp Technology, Department of Fiber and Polymer Technology, KTH Royal Institute of Technology, Teknikringen 56-58, 100 44, Stockholm, Sweden

[4] Commodity Science and Customs Affairs Department, State University of Trade and Economics, Kyoto St., 19, 02156 Kyiv, Ukraine

* Correspondence: d.baklan@kpi.ua (D.B.); olena@kth.se (O.S.); Tel.: +380505144988 (D.B.); Tel.: +46767762735 (O.S.)

Abstract

This work presents an approach to water-dispersible polylactide (PLA) particle fabrication and their application in low-temperature film formation using a combination of mechanical dispersion and ultrasonication techniques. Stable PLA dispersions were obtained after removal of surfactant and allowed for the preparation of thin films exhibiting significantly reduced minimum film-formation temperature (MFFT), particularly when plasticized. To tailor the interfacial behavior and mechanical flexibility of the resulting coatings, a set of conventional and bio-based plasticizers was evaluated, including epoxidized fatty acids, PEG-400, and several hydrophobic deep eutectic solvents (HDES) synthesized from menthol and carboxylic acids. Compatibility between PLA and each plasticizer was predicted using Hansen solubility parameters, and the efficiency of plasticization was assessed through glass-transition temperature suppression in solvent-cast films. The combination of submicron PLA particles and selected plasticizers enabled film formation at temperatures as low as 48 °C, confirming the potential of these systems for energy-efficient coating technologies. Furthermore, composite coatings incorporating micro sized cellulose fibers regenerated from agricultural residues were successfully obtained, demonstrating the feasibility of integrating bio-derived fillers into waterborne PLA formulations. This study highlights the use of water-insoluble ionic-liquid-type plasticizers for PLA dispersions and establishes a foundation for developing sustainable, low-VOC, and low-temperature PLA-based coating materials.

Keywords: polylactide; polymer; water dispersion coatings; polymer film; coating; glass transition temperature

1. Introduction

The transition from fossil hydrocarbon-based polymers to bio-based and optionally biodegradable materials is one of the significant routes of carbon footprint reducing of plastic, composites, packaging (including high volume food and personal care), and coatings industrial branches [1,2]. Contemporary, industrially established bioplastics include polylactide (PLA), microbial polyhydroxyalkanoates (PHAs; e.g., PHB/PHBV), and poly(butylene succinate) (PBS), with polyethylene furanoate (PEF) emerging for packaging. Authoritative overviews detail their production routes, properties, and markets [3–8]. Many leading bioplastics, especially PHAs, are synthesized intracellularly by bacteria via fermentation and recovered from biomass rather than by

 doi:10.20944/preprints202511.1672.v1

synthetic emulsion polymerization, which explains why "emulsion routes" are generally inapplicable to their primary manufacture [9]. We focus our research on PLA because it couples a mature, large-scale supply chain, robust melt processability and property tunability, and broad end-of-life options at competitive cost [3,10]. One possible approach to producing coatings from such bioplastics is the use of their solutions in organic solvents. However, this strategy conflicts with the principles of green chemistry, specifically the reduction of VOC emissions, as well as with relevant regulatory frameworks (i.e., Industrial Emissions Directive 2010/75/EU). Using aqueous dispersions is the most promising strategy for addressing this challenge. Such dispersions can be obtained from polymer solutions, for example via the solvent-evaporation method. This approach is particularly advantageous for polymers such as PLA or PBS because it allows dispersion formation under mild conditions without subjecting the polymer to thermal degradation, while also enabling high solids content and narrow particle-size distributions. Concentrated PLA and PHA dispersions (20–40 wt. %) have been successfully prepared through controlled solvent evaporation, demonstrating good film-forming ability and stability [11–13]. Importantly, all handling of organic solvents occurs at the production stage rather than during coating application, ensuring effective capture, recycling, and regulatory compliance under industrial emission control standards.

Most bio-based polymers have relatively high glass transition temperatures, which makes them brittle materials unsuitable for direct film formation. [14]. To overcome this disadvantage, plasticizers are used, which, by replacing intermolecular interactions of the polymer with interactions with more mobile molecules, increase the segmental mobility of polymers and, consequently, reduce the brittleness of the material. [15,16]. The most common plasticizers used in PLA formulations intended for extrusion are polyethylene glycol (PEG) [17], citrate esters, especially acetyl tributyl citrate (ATBC) and triethyl citrate (TEC) [18], oligomeric lactic acid, etc. [16].Ionic liquids are promising plasticizers for polylactide [19] because their highly tunable polarity, low volatility, and strong specific interactions with ester groups [20–22]. In addition to compatibility with the polymer, plasticizers used in water-dispersion coating technology must also be insoluble in the aqueous phase [23–25]. On the one hand, this will ensure uniform film formation, and on the other hand, it will prevent plasticizer migration when in contact with moist environments. Therefore, plasticizers such as PEG are unsuitable for these applications.

An additional feature of polymer dispersion coating technology is the process of film formation through the fusion of dispersion particles. As shown in [26], particle fusion occurs when the dispersion medium (water) evaporates due to the capillary pressure that arises between the particles. The capillary pressure magnitude depends mainly on the capillary diameter. However, capillary pressure is not all that is needed to form a film, the polymer particle material itself must be soft enough to deform, due to mobility of macromolecular segments. This softness depends on the ambient temperature and determines the minimum temperature at which the film is formed. The value of this temperature is always higher than the glass transition temperature of the material. Obviously, to use polylactide dispersions as a substitute for traditional water-dispersible binders, this temperature should be below 5 °C. An alternative may be intermediate technology that partially uses additional heating for coalescence, which is widely used in powder paints [27].

An additional factor determining the applicability of dispersions is the possibility of compounding them with various functional additives: reinforcing fillers, pigments, which must form a monolithic structure with the film-forming phase after curing.

The problem of this study is the need to obtain such aqueous polylactide dispersions that can form a film at temperatures as close as possible to the ambient temperature and can be compounded. To solve this problem, the influence of plasticizers, including promising ionic liquids, on the reduction of the glass transition temperature and the minimum film formation temperature, as well as the reduction of these indicators by decreasing the particle size, is being investigated. The work also demonstrates the formation of composites based on film formers and reinforcing cellulose fillers from agricultural waste.

 doi:10.20944/preprints202511.1672.v1

2. Materials and Methods

The research structure (Figure 1) included an analytical selection of the most suitable polylactide plasticizers from the class of ionic liquids, followed by the synthesis of selected samples, for which water solubility was experimentally evaluated. For the synthesized samples and benchmark plasticizers, the effect of the glass transition temperature reduction was determined. The next important stage was to determine the possibility of reducing the particle size by modifying the production modes (mechanical dispersion and ultrasound). Next, the influence of two main factors (plasticization + dispersion particle size) on the film formation temperature was considered. The final stage of the work was to determine the possibility of introducing reinforcing fillers into the polylactide films formed from the dispersion.

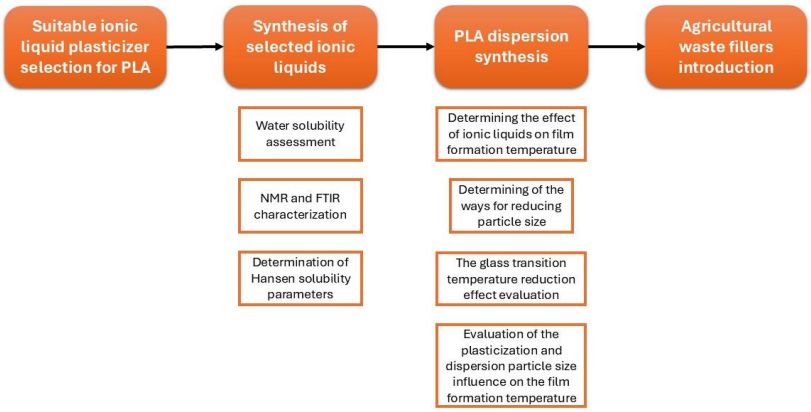

Figure 1. The research structure scheme.

2.1. Materials

The Ingeo Biopolymer 4060D (NatureWorks, Minnetonka, MN, USA) Polylactide (PLA) was used in this work. This PLA grade was selected because its amorphous structure produces a relatively low glass-transition temperature (55–60 °C), which improves its suitability for use in films. A few ionic liquids were selected as plasticizers Menthol-Levulinic acid 1:1 (MenLev), Menthol-Acetic acid 1:1 (MenAc), Menthol-Lactic acid 1:1 (MenLac), Menthol-Oleic acid 1:1 (MenOl), Menthol-Linalool 1:1 (MenLil). Epoxy oleic acid, Epoxy linoleic acid и PEG-400 were chosen as a reference. Epoxy oleic acid and Epoxy linoleic acid were synthesized according to the methodology described in our previous paper [28]. Dichloromethane was used as a solvent for PLA (Thermo Fisher Scientific, Waltham, MA, USA).

2.2. Obtaining Polylactide Dispersions

The method for obtaining PLA dispersion consisted of the following steps (Figure 2). First, 0.21 g of sodium dodecyl sulfate (SDS) was dissolved in 53.6 g of distilled water using a top stirrer. Next, after complete dissolution, 50 g of a 2.5 wt. % solution of PLA 4060D in dichloromethane was gradually added to the solution. Mixing at this stage was performed using a WiseTis HG 15A high-speed disperser (Daihan Scientific, Daejeon, Korea) at a speed of 27000 rpm for 2 minutes. The dispersion was then transferred to an ultrasonic bath and subjected to ultrasonic treatment for 30 minutes, with the dispersion temperature maintained below 25 °C to minimize dichloromethane evaporation. The treatment parameters were 35 kHz and 50 W.

Complete removal of dichloromethane was performed using an RV 3 V rotary evaporator (IKA, Staufen, Germany). The water bath temperature was set to 40 °C. A slight vacuum was applied to accelerate the removal of dichloromethane. The process was considered complete when water began to be removed. Dichloromethane was used because of its high evaporation rate. The resulting particles were separated by centrifugation and dried on an adhesive coating at room temperature.

 doi:10.20944/preprints202511.1672.v1

This resulted in nanometer-sized PLA particles suitable for further modification and use in film materials. A vacuum drying oven (SV-80, UOSlab, Kyiv, Ukraine) at a temperature of 40 °C and full vacuum was used to concentrate the PLA dispersion for rapid water removal.

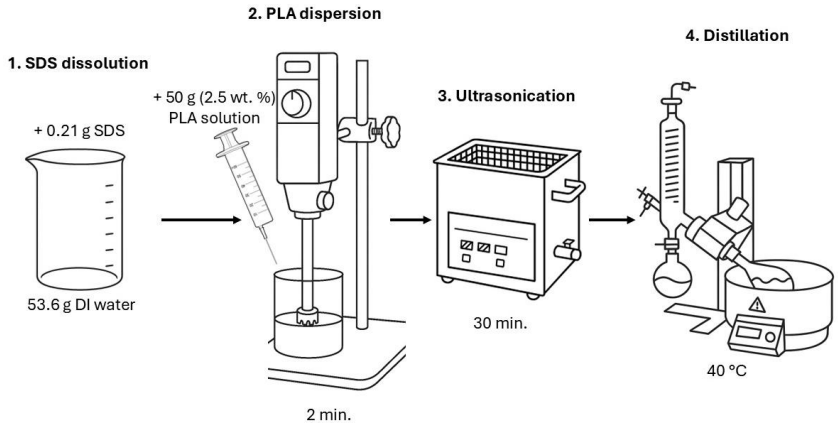

Figure 2. Polylactide dispersion preparation procedure.

2.3. Biofillers Obtaining

Agricultural waste was used to obtain biofillers. Initially, corn stalks and sunflower shell hulls were cut into flakes up to 1 mm long, and coconut shells were first crushed in a jaw crusher and then, when the particle size reached several millimeters, further crushed in a hammer crusher. The chemical treatment of the fibers was the same for both materials. The fillers were treated with a mixture of acetic acid and hydrogen peroxide in a volume ratio of 70:30 for two hours at a temperature of 95 °C, after which they were cooled. They were then immersed in a 0.1 M potassium hydroxide solution for two days at room temperature, after which they were treated with hydrogen peroxide. After chemical treatment, the materials were passed through an FDM-Z-150 colloid mill (Vektor, Guangzhou, China) and then through a blender. The ground particles were sieved through sieves under running water to obtain a particle size in the range of 30-400 μm. Polymethylhydrosiloxane (XIAMETER MHX-1107, Dow Chemical, Midland, MI, USA) was used to hydrophobize the fillers. For this purpose, the fibers were placed in a 1 wt. % solution of the polymethylhydrosiloxane for 3 hours. The fibers were then washed with xylene and kept at a temperature of 130 °C to fix the siloxane on the surface of the cellulose fibers.

2.4. Characterization Methods

For particle characterization an optical microscopy was used (Konus Academy optical microscope with UCMOS 1300 digital camera (Sigeta Optics, Kiev, Ukraine; ver. 4.11.23945.2023.1121, ToupTek, Hangzhou, Zhejiang, China). The surface topography of the obtained films was examined using a MIRA3 SEM (Tescan, Brno, Czech Republic).

Glass transition temperature was examined using the DSC method (PT1000 DSC, Linseis, Selb, Germany). Film formation temperature was examined using a precision heat plate and a microscope.

For ionic liquids analysis ^{1}H NMR was used. HDESs were dissolved in a deuterated solvent to prepare the NMR sample. Chemical analysis was performed via ^{1}H NMR spectroscopy (400 MHz, Bruker Avance III HD 400 MHz, with a 5 mm broadband probe). Each spectrum was recorded with 120 scans and 48 K data points. To confirm the theoretically predicted interaction through the functional reactive groups of the compounds, FTIR spectra were obtained using a IRSpirit spectrometer (Shimadzu, Kyoto, Japan) with spectral resolution of 4 cm^{-1} in the range of 400–4000 cm^{-1}. FTIR spectroscopy in ATR mode (IRSpirit, Shimadzu, Kyoto, Japan) was used for PLA film analysis.

Hansen solubility parameters were used to model the compatibility of plasticizers with polymers. Hansen's theory includes three interactions between molecules: δ_d (dispersion forces energy); δ_p (dipolar intermolecular forces energy); δ_h (hydrogen bonds energy). HSP is measured

 doi:10.20944/preprints202511.1672.v1

using the sphere method, where the center of the sphere has the HSP coordinates of the polymer under study, and the radius determines the limits of its compatibility. According to the Hansen model, the radius ratios of the plasticizer (R_a) and polymer (R_o) spheres are a condition for their compatibility. The Relative Energy Difference (RED) parameter is the ratio of R_a/R_o (If RED>1, the plasticizer is incompatible with the polymer; if RED<1, it is compatible).

Hansen solubility parameters for ionic liquids were determined using solvents (water, dichloromethane, isopropyl alcohol, hexane, ethyl acetate, n-butanol, cyclohexane, dimethylformamide, o-xylene, and dimethyl sulfoxide or their mixtures). For experiments dichloromethane was used as a solvent. All named substances were purchased from the local supplier HLR Ukraine (Chemlaborreactiv LLC, Brovary, Ukraine).

The solubility borders and sphere centers in D, P, H coordinates (Hansen sphere calculation) were calculated using the HSP Excel spreadsheet prepared by Dr. Diaz de los Rios [29,30].

3. Results and Discussion

The Hansen solubility parameters were employed to predict the compatibility of the ionic liquids with the biopolymers. The source of data for ionic liquids was the publication [31], that contains these parameters defined with empirical and semi-empirical approaches. As authors conclude, for the dispersion component δ_d all approaches give close values, for δ_p – the Hoftyzer and Van Krevelen model provides the best accuracy and δ_h can be predicted directly only with a large error. Thus, it is recommended to calculate the last parameter using δ_t, which can be done using equation (1):

$$\delta_h = \sqrt{\delta_t^2 - \delta_d^2 - \delta_p^2}, \quad (1)$$

From the full set of ionic liquids, as nonpolar candidates Menthol-Levulinic acid (1:1) and Menthol-Acetic acid (1:1) were selected. Although solubility parameters for Menthol-Lactic acid (1:1) were not found in the literature, its presumed low polarity and the affinity of the hydrogen-bond acceptor (lactic acid) for the monomeric unit of the polymer to be plasticized justified the inclusion of this HDES in the analysis. All synthesized HDES were tested on the water solubility, and it was surprisingly found that, despite the relative non-polar hydrogen bond donor menthol, they are water soluble. As was mentioned before, this property may cause the leaching of plasticizer in moist environments (especially from thin layer films), moreover, the plasticizer solution in water may be absorbed by the porous substrates after application and PLA/plasticizer ratio will decrease. To overcome this issue, two water-insoluble plasticizers from our previous work were utilized (epoxidized oleic and linoleic acids), and an additional HDES, Menthol-Oleic acid (1:1), was synthesized. This ionic liquid is not water-soluble and forms dispersions under mechanical stirring, which may be stabilized with SDS (like PLA dispersions). The PEG-400 plasticizer was taken into analysis as a benchmark.

3.1. NMR and FTIR Characterization of HDES

For hydrophobic deep eutectic solvents (HDES), ^{1}H NMR spectroscopy was selected due to its ability to track the presence and strength of hydrogen bonds, the degree of association between the hydrogen bond donor and acceptor, and possible conformational changes. For HDES, which often includes nonpolar and weakly interacting molecules, ^{1}H NMR can detect subtle shifts in the proton environment that indicate the formation of a eutectic network. This information is essential for understanding the stability, miscibility, and physicochemical behavior of HDES. FTIR spectroscopy complements ^{1}H NMR because it provides direct evidence of interactions between specific functional groups that NMR cannot fully reveal. ^{1}H NMR allows changes in the electronic environment of protons to be determined, while FTIR detects vibrations associated with hydrogen bonds in –OH, –NH, and C–H groups.

Analysis of FTIR spectra (Figure 3) of HDES based on Menthol-Levulinic acid, Menthol-Acetic acid, Menthol-Lactic acid, and Menthol-Oleic acid shows a broad O–H stretching band around 3600–

 doi:10.20944/preprints202511.1672.v1

3200 cm^{-1}, indicating the presence of a hydrogen bond between the hydroxyl group of menthol and the carboxyl group of organic acids. The high-intensity peak 1710–1730 cm^{-1} indicates stretching vibrations of the C=O bonds of the carboxyl group in the acid. Additionally, the FTIR spectrum shows peaks corresponding to C–O bonds at 1180–1040 cm^{-1} and C–H bonds at 2910–2930 cm^{-1}.

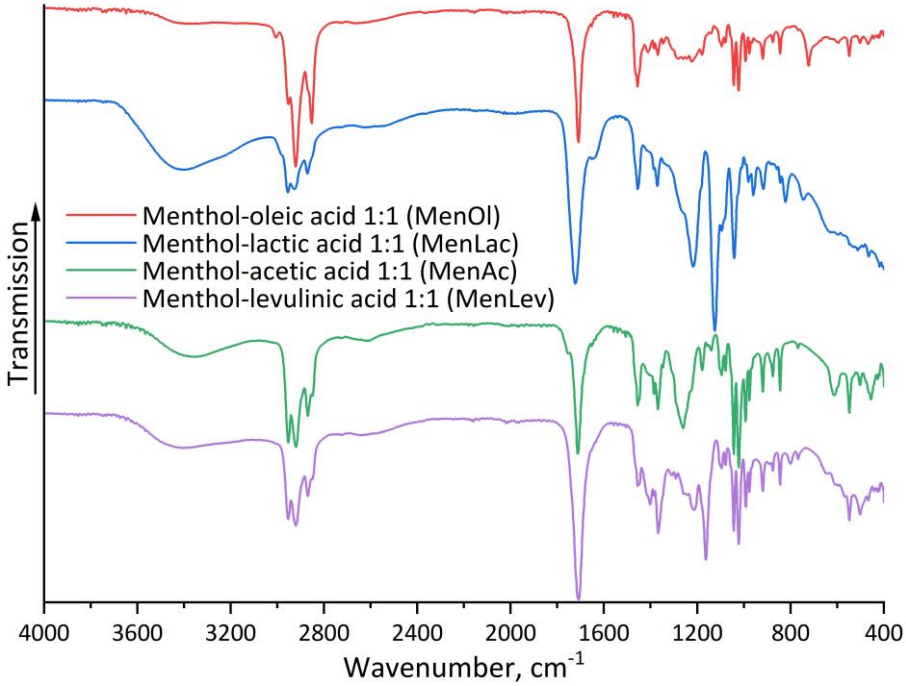

Figure 3. FTIR spectra of HDES.

For all obtained HDES ^{1}H NMR spectra (400 MHz, $CDCl_3$) (Figure 4) showed a series of signals at δ 0.80–1.10 (m, CH_3 menthol), 1.20–2.20 (m, CH_2). For Menthol-Levulinic acid, peaks at 2.45 (t, CH_2–CO), 3.35 (m, CH–OH), 4.10 (m, CH–O), and 9.70 (s, COOH) are present, which is consistent with the proposed composition and confirms the formation of hydrogen bonds in HDES. Similarly, for HDES Menthol-Acetic acid, there are peaks at 2.08 (s, CH_3CO), 3.35 (m, CH–OH), 4.10 (m, CH–O) and 11.30 (s, COOH), and for HDES of Menthol-Lactic acid, 3.35 (m, CH–OH menthol), 4.15 (q, CH–OH lactic acid) and 9.75 (s, COOH). Finally, for DES menthol and oleic acid, there are δ 0.88 (t, 3H, CH_3 oleic acid), 1.20–1.35 (m, $(CH_2)_n$ oleic chain), 1.98–2.05 (m, allyl CH_2 adjacent to C=C), 2.30–2.40 (t, ^{2}H, CH_2–CO oleic acid), 3.30–3.40 (m, CH–OH menthol), 4.05–4.15 (m, oxygenated menthol methine, if present), 5.30–5.40 (m, ^{2}H, vinyl CH of oleic acid) and 10.8–11.8 (broad s, COOH, hydrogen bond).

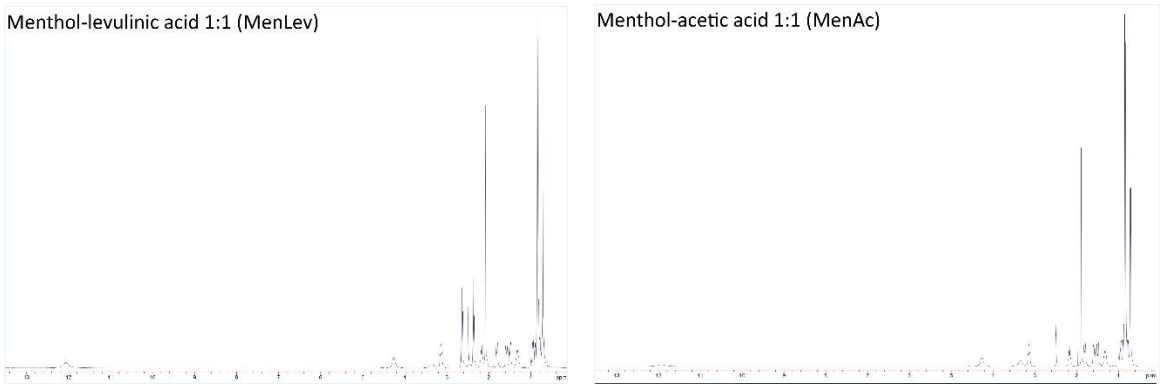

(**a**) (**b**)

 doi:10.20944/preprints202511.1672.v1

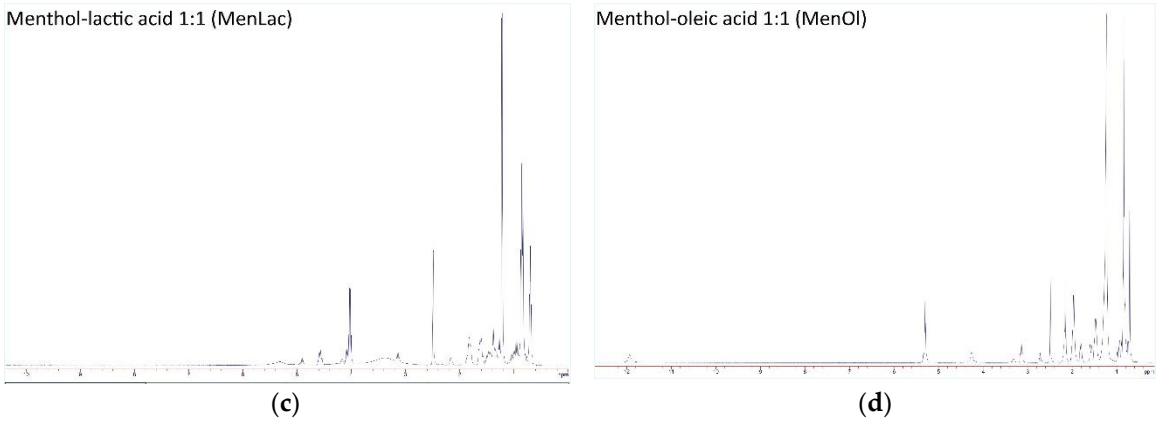

Figure 2. ^{1}H NMR spectra of HDES: (**a**) MenLev; (**b**) MenAc; (**c**) MenLac; (**d**) MenOl.

To assess the compatibility between all selected and synthesized plasticizers and polylactide, the HSP calculations were performed (Table 1). As can be seen, the RED values of all pairs (Plasticizer – PLA) are less than 1, indicating compatibility. It may also be noted that the lowest values of RED are shown by epoxidized oleic and linoleic acids and the highest values, for MenAc and MenLac, respectively. On the other hand, the benchmarking PEG-400 has a moderate value of RED.

Table 1. Hansen solubility parameters of plasticizers and PLA polymer.

Title 1	δd	δp	δh	R_0	R_a	RED	Ref.
Menthol-Levulinic acid 1:1 (MenLev)	17.15	5.17	10.96		6.7	0.79	[31]
Menthol-Acetic acid 1:1 (MenAc)	16.88	4.15	11.60		7.8	0.92	[31]
Menthol-Lactic acid 1:1 (MenLac)	16.7	2.5	8.8		7.8	0.92	-
Menthol-Oleic acid 1:1 (MenOl)	16.8	5.0	9.4		5.8	0.68	-
Epoxy oleic acid	16.6	11.1	9.8		3.6	0.42	[28]
Epoxy linoleic acid	16.6	11.4	10.5		4.4	0.51	[28]
PEG-400	14.6	7.5	9.4		5.4	0.64	[32]
PLA 4060D	16.5	9.9	6.4	8.5			[28]

FTIR spectroscopy revealed no significant changes in the chemical composition (Figure 5), confirming the absence of covalent interactions between the polymer and plasticizer.

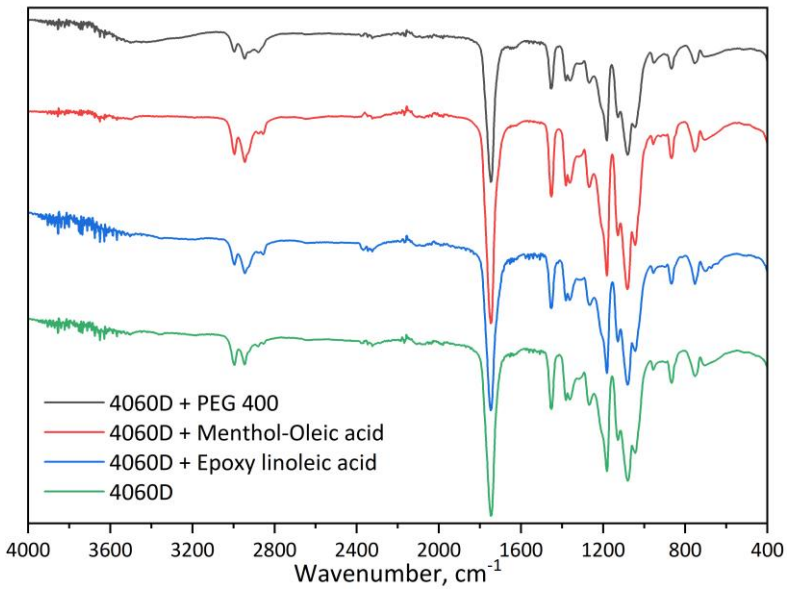

Figure 5. FTIR spectra of PLA-plasticizer compositions.

 doi:10.20944/preprints202511.1672.v1

The effectiveness of the plasticizer is commonly assessed by the grade of the polymer glass transition temperature depression. The nature of this effect lies in the increase of segmental mobility of polymer molecules in case the compatible lower molecular weight plasticizer is introduced between chains or their supramolecular arrangements [33]. The T_g suppression in this work was determined with DSC technique (Figure 6) on polymer-plasticizer (20 wt. %) mixtures, which were cast in form of films from dichloromethane solutions and after complete drying at 50 °C for 1,5 h and chilling to room temperature in a dry chamber. The T_g of 4060D polymer is 62 °C, which is slightly higher than an interval stated in TDS (55-60 °C), but coincides with the measured in [34].

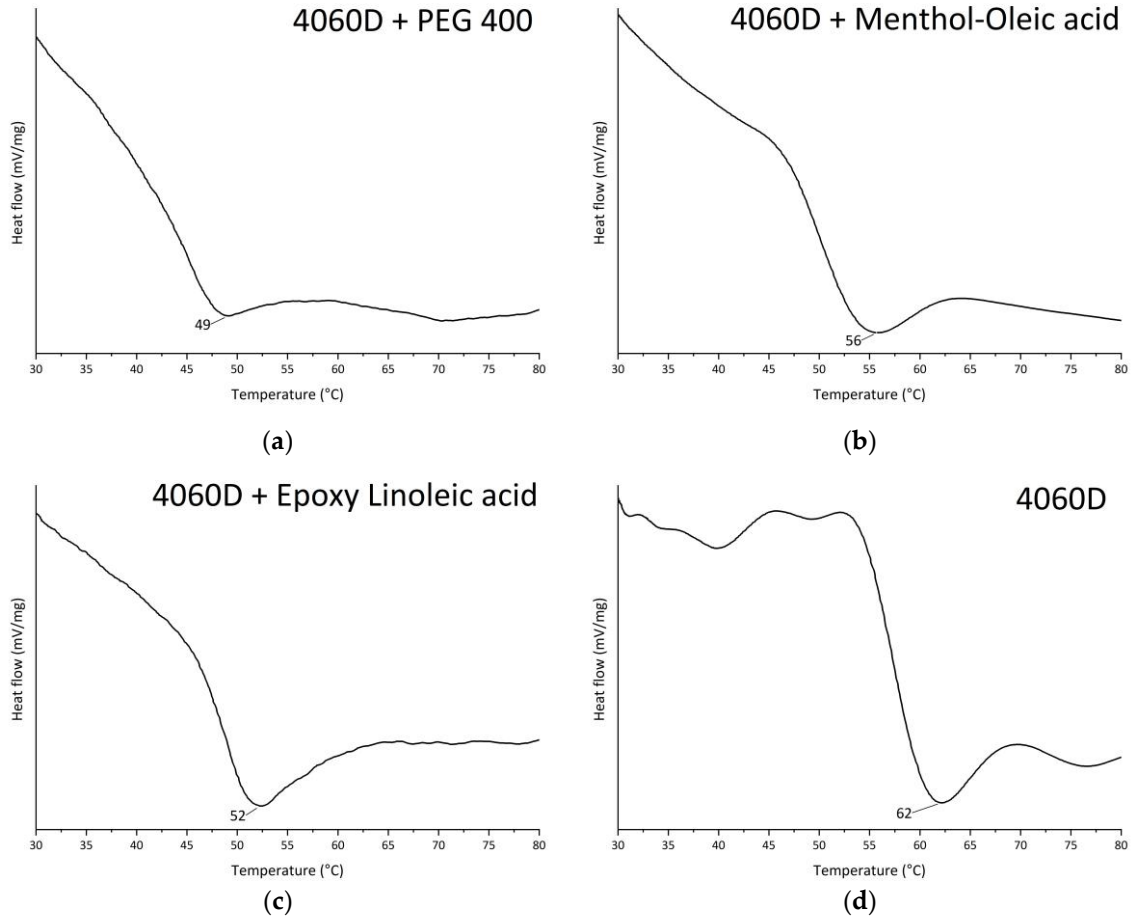

Figure 6. DSC results for PLA and its plasticates: (**a**) 4060D plasticized with 20 wt. % PEG-400; (**b**) 4060D plasticized with 20 wt. % MenOl; (**c**) 4060D plasticized with 20 wt. % Epoxy Linoleic acid; (**d**) neat 4060D.

PEG-400 effect is the most significant among all the plasticizers considered: the T_g lowers by 17 °C, in case of the epoxidized linoleic acid the decrease is 10 °C and the MenOl gives only 6 °C. Such T_g suppression only generally correlates with the HSP affinity prediction the substances considered are effective in T_g suppression, indicating the approximation of such analysis. A similar conclusion may be found in [35], where it was shown that HSP may be the indicator of the miscibility in general, however, the structural factors play the crucial role in T_g suppression. In [36] the phenomenon of antiplastification is considered for the highly compatible pairs of polymer-plasticizers, again. accounting on the structure features of interacting molecules. In [37] It is shown, in addition, that the affinity predicted by HSP is true for the certain plasticizer content range.

The PLA particle formation by the solvent evaporation method was performed using the mechanical dispersion of the solution of PLA in dichloromethane in water, supported with the addition of SBS surfactant and additional ultrasonication. The effectiveness of ultrasonication is determined by the dispersed phase viscosity balance and the energy density, which is provided by the ultrasonic homogenizer. In our experiments with a low power homogenizer (60 Wt) it was noted

 doi:10.20944/preprints202511.1672.v1

that only at the concentration of 2.5 wt. % of polymer was the submicron fraction formed (Figure 7). It was stated in [37] that at higher ultrasonic energy density, it is possible to homogenize more concentrated solutions. As may be seen from Figure 7, the mechanical stirring itself is able to deliver particles with 4.5 μm average diameter and ultrasonication results in a decrease in this value to 1.5 μm. Together with this, the submicron fraction appears.

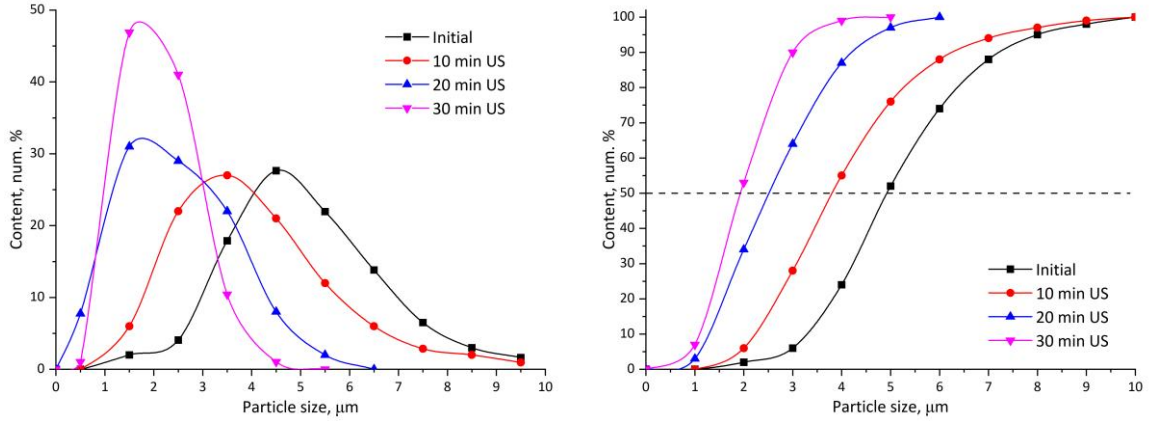

(**a**) (**b**)

Figure 7. Distribution of emulsion particle size: (**a**) differential; (**b**) cumulative.

As it was recently shown by Belletti group [38], using the combination of the mechanical dispersion + ultrasound treatment, the stable dispersions of 200–500 nm particle size PLA may be obtained. In our work, after the fabrication of stable dispersions, they were washed off the stabilizing surfactant through centrifugation. It was found that during this process, it is possible to separate a fine fraction of PLA particles as well.

In Figure 3 comparative images of particles obtained by mechanical dispersion (Figure 8a) and their combination with 30 min ultrasonication + centrifugal separation (Figure 8b). The samples were free of solvent, obtained by casting dispersion onto the glass, drying at ambient (20 ±2 °C) temperature, RH 30 ±5%. As may be noticed, the particle size on Figure 9a and 9b differs in at least order. In the first case, there are particles of average size 2.2 μm, and in the second case – 140 nm. It may be noted also the difference between micro (Figure 8a) and nano (Figure 8b) particles in the sintering of later even at ambient conditions, that may be seen from the image. However, the complete coalescence of particles does not happen and requires further measures.

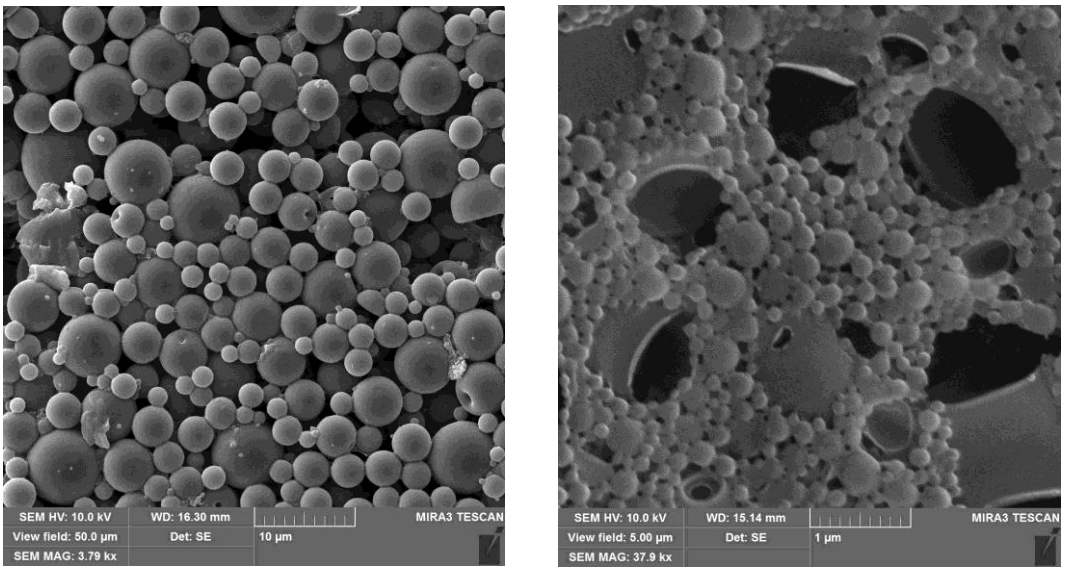

(**a**) (**b**)

 doi:10.20944/preprints202511.1672.v1

Figure 8. PLA suspensions particles: (**a**) formed with mechanical homogenization; (**b**) formed with a combination of ultrasonic and mechanical homogenization.

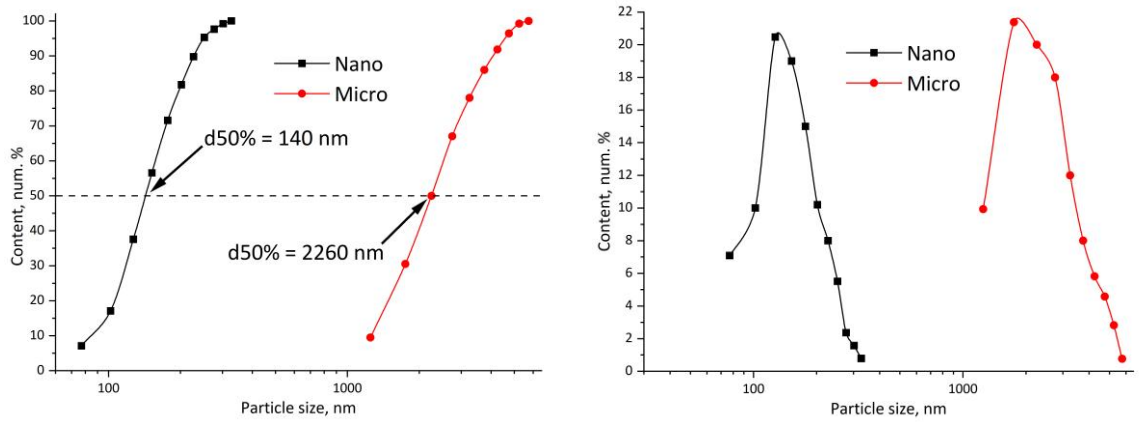

(**a**) (**b**)

Figure 9. Particle size distribution of dispersions obtained by mechanical + ultrasonic dispergation (Nano) and mechanical dispergation (Micro): (**a**) differential; (**b**) cumulative.

As can be seen from Figure 10, the minimum film formation temperature is significantly affected by the plasticizer addition. Even the less effective MenAc decreases its value for microparticle dispersion by 23 °C. The most effective MenLac by 43 °C at 20 wt. % content. The particle size reduction and the following reduction of the capillary diameter increase the coalescence force and, as a result, suppress the minimum temperature of transparency. The 2.2 mm and 140 nm particles differ in more than one order in size, which lowers the MFFT from 128 °C to 80 °C. The addition of plasticizers in this case is also effective: the MenLac provides a film formation at 48 °C, and MenOl and PEG-400 have a comparable effect. It is worth mentioning that the MFFT and T_g are close in this case, so it may be assumed that the plastification effectiveness is close to its theoretical threshold limited by T_g if the particles are fine enough.

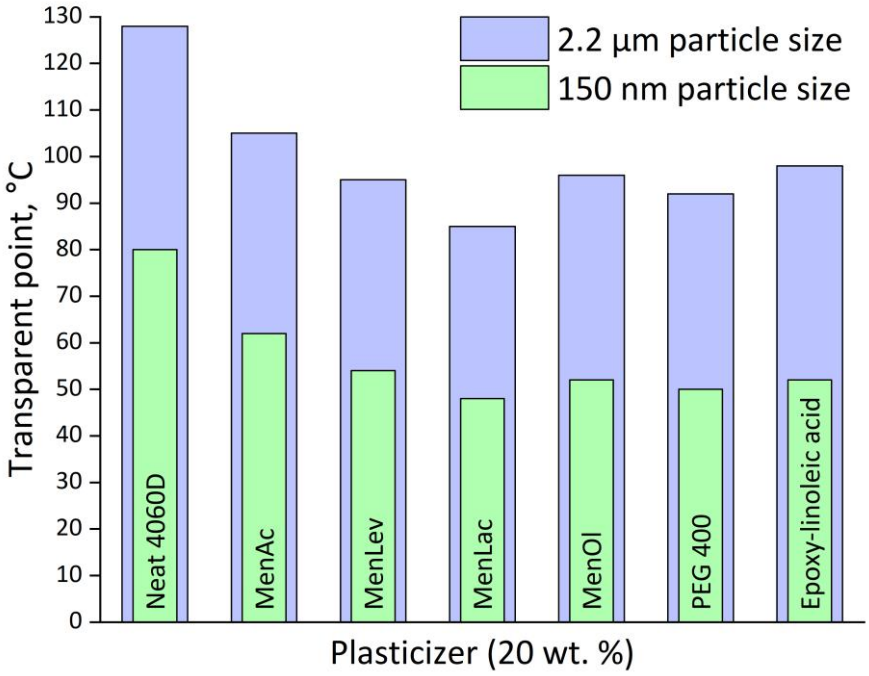

Figure 10. Film formation temperature (transparency point) for PLA water dispersions.

 doi:10.20944/preprints202511.1672.v1

In the design of technologically mature coatings derived from disperse particles, whether aqueous dispersions or powder-based systems, the ability of particles to coalesce with other components of the formulation, particularly their capacity to wet the surface of fillers, remains a critical requirement. In the present study, fillers originating from agricultural waste, specifically sunflower seed husks, corn stalks, and coconut shells, were investigated. As demonstrated in Figure 11a and 11b, the first two sources enable the production of cellulose-based fibrous particles with an L/D ratio of 10.5 ±0.5 and 11.5 ±0.5 respectively, indicating their potential for use as reinforcing agents and shrinkage-reducing fillers. The particles produced from coconut shells (Figure 11c) (L/D ratio = 8.5 ±0.4) exhibit characteristics more consistent with inert fillers within the system.

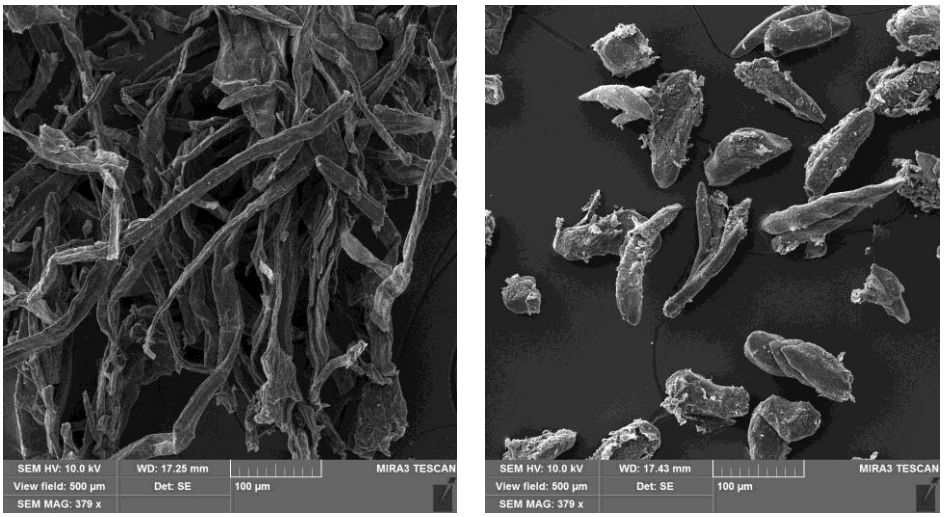

(**a**) (**b**) (**c**)

Figure 11. Natural fibers from agricultural waste: (**a**) sunflower seed hulls; (**b**) cornstalk; (**c**) coconut shell.

Cellulose-based fibrous fillers possess intrinsically polar surfaces: the free surface energy coordinates at 23 °C are typically γ_S^D≈38–40 mN/m^{-1} and γ_S^P≈8.6–12.6 mN/m^{-1} (total surface energy is ≈ 48–51 mN/m^{-1}) [39]. By contrast, polylactide (PLA) is much less polar, with PLA-film coordinates γ_S^D≈32.8 mN/m^{-1} and γ_S^P≈5.8 mN/m^{-1} (total surface energy is ≈ 38.6 mN/m^{-1}) [40]. Reducing the polarity of cellulose via silane treatments narrows this mismatch and thermodynamically improves PLA wetting/adhesion by lowering the polar contribution to the interfacial tension. Because PLA ester backbone undergoes moisture-catalyzed hydrolysis that accelerates with temperature and humidity, causing rapid molecular-weight loss and deterioration of mechanical properties during processing and service, silanization may be a measure to limit such processes [41,42]. Moreover, reducing the polarity of cellulose surfaces suppresses inter-particle hydrogen bonding and agglomeration, which lowers the melt viscosity of PLA - cellulose composites and markedly improves their processability during extrusion and molding [43]. Another remarkable effect is the reduction of interfacial water accumulation in PLA composites, thereby limiting hydrolysis-driven embrittlement and enhancing both the long-term durability and dimensional stability of the material under humid conditions [44]. In our study, the silanization of the obtained cellulose fibers helped to decrease the moisture uptake by compositions from 3.30 to 3.02 wt. % (coconut), from 3.6 to 2.80 wt. % (cornstalk) and from 3.50 to 2.96 wt. % (sunflower seed hulls). The distribution of the fibers inside the sintered particle polylactide matrix (Figure 12) is even without clogs (which are usual in the case of fiber-matrix incompatibility).

In the case of cornstalk, the refined particles form a net-like interconnection, making it a suitable candidate for the reinforcing filler role. Although the particles derived from sunflower seed hulls exhibit a high L/D ratio, their reinforcing potential is lower than that of particles from corn stalks due to the presence of non-fibrous impurities. The coconut shell–derived particles are more suitable as fillers for PLA compositions, as they do not contain a sufficiently high fraction of fibrous elements.

 doi:10.20944/preprints202511.1672.v1

Overall, it can be stated that the obtained plasticized PLA dispersions form composite coatings during film formation in combination with cellulose-based fillers derived from agricultural waste.

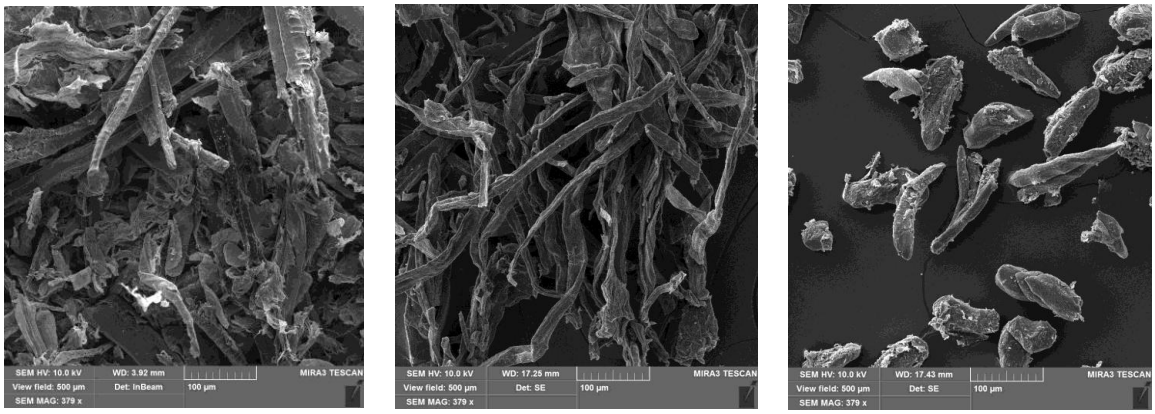

(**a**) (**b**) (**c**)

Figure 12. Distribution of fibers in PLA matrix after particle sintering: (**a**) sunflower seed hulls; (**b**) cornstalk; (**c**) coconut shell.

4. Conclusions

This study demonstrates a viable approach to sustainable waterborne PLA coatings by combining particle-size reduction with tailored plasticization. For the first time, water-insoluble ionic liquid-type plasticizers for PLA were synthesized, including Menthol-Oleic acid (1:1), which overcomes the leaching limitations associated with water-soluble deep eutectic solvents.

Particle size reduction from approximately 2.2 µm (mechanical dispersion) to 140 nm (mechanical plus ultrasonication) decreased the minimum film-formation temperature (MFFT) from 128 °C to 80 °C. Plasticization further reduced the MFFT to 48 °C using Menthol-Lactic acid at 20 wt. %. Differential scanning calorimetry confirmed corresponding glass transition temperature depressions of −17 °C (PEG-400), −10 °C (epoxidized linoleic acid), and −6 °C (Menthol-Oleic acid), consistent with compatibility trends predicted by Hansen Solubility Parameters.

Moreover, the dispersions enabled the fabrication of crack-free composite coatings incorporating cellulose-based fillers derived from agricultural residues. Fiber dimensions (L/D = 10.5–11.5) and silanization treatment improved compatibility and reduced moisture uptake (e.g., corn stalks from 3.6 wt. % to 2.8 wt. %). These results highlight the potential of plasticized PLA dispersions for energy-efficient, low-temperature curing and the integration of bio-derived reinforcement into waterborne coatings.

Overall, this work establishes a scalable foundation for low-VOC, renewable PLA-based coating materials, supporting future developments in sustainable polymer technologies.

Author Contributions: Conceptualization, O.M.; methodology, D.B. and O.M.; validation, O.M. and D.B.; formal analysis, O.M. and D.B.; investigation, O.M. and D.B.; resources, O.M.; data curation, O.M., D.B., V.V.; writing—original draft preparation, O.M. and D.B.; writing—review and editing, O.M., D.B., O.S. and T.K.; visualization, D.B.; supervision, O.M.; project administration, O.M.; funding acquisition, O.M., O.S. and T.K. All authors have read and agreed to the published version of the manuscript.

Funding: This research was funded by Ministry of Education and Science of Ukraine, agreement number PH/53-2024 (26.09.2024) (European Union aid instrument for fulfilling Ukraine's obligations in the Framework Program of the European Union for Scientific Research and Innovation "Horizon 2020"). O.S. and T.K. kindly acknowledge the support from the Swedish Institute (project nr 00237/2025).

Institutional Review Board Statement: Not applicable.

 doi:10.20944/preprints202511.1672.v1

Data Availability Statement: The original contributions presented in this study are included in the article. Further inquiries can be directed to the corresponding author.

Acknowledgments: During the preparation of this manuscript, the authors used ChatGPT (OpenAI), version GPT-5, for icon creation in the scheme of the polylactide dispersion preparation procedure (Figure 2). The authors have reviewed and edited the output and take full responsibility for the content of this publication.

Conflicts of Interest: The authors declare no conflicts of interest.

Abbreviations

The following abbreviations are used in this manuscript:

PLA	Polylactide
MFFT	Minimum film-formation temperature
HDES	Hydrophobic deep eutectic solvent
NMR	Nuclear magnetic resonance
FTIR	Fourier-transform infrared spectroscopy
RED	Relative Energy Difference
PEG	Polyethylene glycol
SDS	Sodium dodecyl sulfate
DSC	Differential scanning calorimetry

References

1. Righetti, G.I.C.; Faedi, F.; Famulari, A. Embracing Sustainability: The World of Bio-Based Polymers in a Mini Review. *Polymers* 2024, 16, 950. https://doi.org/10.3390/polym16070950
2. Cywar, R.M.; Rorrer, N.A.; Hoyt, C.B.; Beckham, G.T.; Chen, E.Y. -x. Bio-Based Polymers with Performance-Advantaged Properties. *Nat. Rev. Mater.* 2021, 7, 83–103, https://doi.org/10.1038/s41578-021-00363-3
3. Naser, A.Z.; Deiab, I.; Darras, B.M. Poly(Lactic Acid) (PLA) and Polyhydroxyalkanoates (PHAs), Green Alternatives to Petroleum-Based Plastics: A Review. *RSC Adv.* 2021, 11, 17151–17196, https://doi.org/10.1039/d1ra02390j
4. Barletta, M.; Aversa, C.; Ayyoob, M.; Gisario, A.; Hamad, K.; Mehrpouya, M.; Vahabi, H. Poly(Butylene Succinate) (PBS): Materials, Processing, and Industrial Applications. *Prog. Polym. Sci.* 2022, 132, 101579, https://doi.org/10.1016/j.progpolymsci.2022.101579
5. J. H. Sanders, J. Cunniffe, E. Carrejo, C. Burke, A. M. Reynolds, S. C. Dey, M. N. Islam, O. Wagner, D. Argyropoulos, Biobased Polyethylene Furanoate: Production Processes, Sustainability, and Techno-Economics. *Adv. Sustainable Syst.* 2024, 8, 2400074. https://doi.org/10.1002/adsu.202400074
6. Hayes, G.; Laurel, M.; MacKinnon, D.; Zhao, T.; Houck, H. A.; Becer, C. R. Polymers without petrochemicals: Sustainable routes to conventional monomers. *Chem. Rev.* 2022, 123, 2609–2734. https://doi.org/10.1021/acs.chemrev.2c00354
7. Goliszek-Chabros, M.; Smyk, N.; Xu, T.; Matwijczuk, A.; Podkościelna, B.; Sevastyanova, O. Lignin Nanoparticle-Enhanced PVA Foils for UVB/UVC Protection. *Sci. Rep.* 2025, 15, 35735, https://doi.org/10.1038/s41598-025-19753-6
8. Goliszek, M.; Podkościelna, B.; Smyk, N.; Sevastyanova, O. Towards Lignin Valorization: Lignin as a UV-Protective Bio-Additive for Polymer Coatings. *Pure Appl. Chem.* 2023, 95, 475–486, https://doi.org/10.1515/pac-2022-1209
9. Anjum, A.; Zuber, M.; Zia, K. M.; Noreen, A.; Anjum, M. N.; Tabasum, S. Microbial production of polyhydroxyalkanoates (phas) and its copolymers: A review of recent advancements. *Int. J. Biol. Macromol.* 2016, 89, 161–174. https://doi.org/10.1016/j.ijbiomac.2016.04.069
10. Khouri, N.G.; Bahú, J.O.; Blanco-Llamero, C.; Severino, P.; Concha, V.O.C.; Souto, E.B. Polylactic Acid (PLA): Properties, Synthesis, and Biomedical Applications – A Review of the Literature. *J. Mol. Struct.* 2024, 1309, 138243, https://doi.org/10.1016/j.molstruc.2024.138243

 doi:10.20944/preprints202511.1672.v1

11. Belletti, G.; Buoso, S.; Ricci, L.; Guillem-Ortiz, A.; Aragón-Gutiérrez, A.; Bortolini, O.; Bertoldo, M. Preparations of Poly(lactic acid) Dispersions in Water for Coating Applications. *Polymers* 2021, 13, 2767. https://doi.org/10.3390/polym13162767
12. Pieters, K.; Mekonnen, T. H. Stable aqueous dispersions of poly(3-hydroxybutyrate-co-3-hydroxyvalerate) (PHBV) polymer for barrier paper coating. *Prog. Org. Coat.* 2023, 187, 108101. https://doi.org/10.1016/j.porgcoat.2023.108101
13. Calosi, M.; D'Iorio, A.; Buratti, E.; Cortesi, R.; Franco, S.; Angelini, R.; Bertoldo, M. Preparation of high-solid PLA waterborne dispersions with PEG-PLA-PEG block copolymer as surfactant and their use as hydrophobic coating on paper. *Prog. Org. Coat.* 2024, 193, 108541. https://doi.org/10.1016/j.porgcoat.2024.108541
14. Nguyen, H.T.H.; Qi, P.; Rostagno, M.; Feteha, A.; Miller, S.A. The Quest for High Glass Transition Temperature Bioplastics. *J. Mater. Chem. A* 2018, 6, 9298–9331, https://doi.org/10.1039/c8ta00377g
15. Sun, S.; Weng, Y.; Zhang, C. Recent Advancements in Bio-Based Plasticizers for Polylactic Acid (PLA): A Review. *Polym. Test.* 2024, 140, 108603, https://doi.org/10.1016/j.polymertesting.2024.108603
16. Mastalygina, E.E.; Aleksanyan, K.V. Recent Approaches to the Plasticization of Poly(Lactic Acid) (PLA) (A Review). *Polymers* 2023, 16, 87, https://doi.org/10.3390/polym16010087
17. Li, D.; Jiang, Y.; Lv, S.; Liu, X.; Gu, J.; Chen, Q.; Zhang, Y. Preparation of Plasticized Poly (Lactic Acid) and Its Influence on the Properties of Composite Materials. PLoS ONE 2018, 13, e0193520, https://doi.org/10.1371/journal.pone.0193520
18. Harte, I.; Birkinshaw, C.; Jones, E.; Kennedy, J.; DeBarra, E. The Effect of Citrate Ester Plasticizers on the Thermal and Mechanical Properties of Poly(DL--lactide). *J. Appl. Polym. Sci.* 2012, 127, 1997–2003, https://doi.org/10.1002/app.37600
19. Shamshina, J.L.; Berton, P. Ionic Liquids as Designed, Multi-Functional Plasticizers for Biodegradable Polymeric Materials: A Mini-Review. *Int. J. Mol. Sci.* 2024, 25, 1720. https://doi.org/10.3390/ijms25031720
20. Rebelo, L.P.N.; Lopes, J.N.C.; Esperança, J.M.S.S.; Filipe, E. On the Critical Temperature, Normal Boiling Point, and Vapor Pressure of Ionic Liquids. *J. Phys. Chem. B* 2005, 109, 6040–6043, https://doi.org/10.1021/jp050430h
21. Rooney, D.; Jacquemin, J.; Gardas, R. Thermophysical Properties of Ionic Liquids. *Top. Curr. Chem.* 2009, 290, 185–212, https://doi.org/10.1007/128_2008_32
22. Dutkowski, K.; Kruzel, M.; Smuga-Kogut, M.; Walczak, M. A Review of the State of the Art on Ionic Liquids and Their Physical Properties during Heat Transfer. *Energies* 2025, 18, 4053, https://doi.org/10.3390/en18154053
23. Chaos, A.; Sangroniz, A.; Fernández, J.; del Río, J.; Iriarte, M.; Sarasua, J. R.; Etxeberria, A. Plasticization of poly(lactide) with poly(ethylene glycol): Low weight plasticizer vs triblock copolymers. effect on free volume and barrier properties. *J. Appl. Polym. Sci.* 2019, 137. https://doi.org/10.1002/app.48868
24. Mohammed, A.A.B.A.; Hasan, Z.; Omran, A.A.B.; Elfaghi, A.M.; Khattak, M.A.; Ilyas, R.A.; Sapuan, S.M. Effect of Various Plasticizers in Different Concentrations on Physical, Thermal, Mechanical, and Structural Properties of Wheat Starch-Based Films. *Polymers* 2023, 15, 63. https://doi.org/10.3390/polym15010063
25. Jarray, A.; Gerbaud, V.; Hemati, M. Polymer-plasticizer compatibility during coating formulation: A multi-scale investigation. *Prog. Org. Coat.* 2016, 101, 195–206. https://doi.org/10.1016/j.porgcoat.2016.08.008
26. Arjmandi, A.; Bi, H.; Nielsen, S. U.; Dam-Johansen, K. From wet to protective: Film formation in Waterborne Coatings. *ACS Appl. Mater. Interfaces.* 2024, 16, 58006–58028. https://doi.org/10.1021/acsami.4c09729
27. Yomo, S. Curing Behavior of Waterborne Paint Containing Catalyst Encapsulated in Micelle. *Coatings* 2021, 11, 375. https://doi.org/10.3390/coatings11040375
28. Myronyuk, O.; Baklan, D.; Bilousova, A.; Smalii, I.; Vorobyova, V.; Halysh, V.; Trus, I. Plasticized Polylactide Film Coating Formation from Redispersible Particles. *AppliedChem* 2025, 5, 14. https://doi.org/10.3390/appliedchem5030014
29. De Los Ríos, M.D.; Belmonte, R.M. Extending Microsoft Excel and Hansen Solubility Parameters Relationship to Double Hansen's Sphere Calculation. *SN Appl. Sci.* 2022, 4, 185

30. De Los Ríos, M.D.; Ramos, E.H. Determination of the Hansen Solubility Parameters and the Hansen Sphere Radius with the Aid of the Solver Add-in of Microsoft Excel. *SN Appl. Sci.* 2020, 2, 676
31. Fernandes, C.C.; Paiva, A.; Haghbakhsh, R.; Duarte, A.R.C. Application of Hansen Solubility Parameters in the Eutectic Mixtures: Difference between Empirical and Semi-Empirical Models. *Sci. Rep.* 2025, 15, 3862, https://doi.org/10.1038/s41598-025-87050-3
32. Alqarni, M.H.; Haq, N.; Alam, P.; Abdel-Kader, M.S.; Foudah, A.I.; Shakeel, F. Solubility Data, Hansen Solubility Parameters and Thermodynamic Behavior of Pterostilbene in Some Pure Solvents and Different (PEG-400 + Water) Cosolvent Compositions. *J. Mol. Liq.* 2021, 331, 115700, https://doi.org/10.1016/j.molliq.2021.115700.
33. Guo, J.; Liu, X.; Liu, M.; Han, M.; Liu, Y.; Ji, S. Effect of Molecular Weight of Poly(Ethylene Glycol) on Plasticization of Poly(L-Lactic Acid). *Polymer* 2021, 223, 123720, https://doi.org/10.1016/j.polymer.2021.123720
34. Gonçalves, F.A.M.M.; Cruz, S.M.A.; Coelho, J.F.J.; Serra, A.C. The Impact of the Addition of Compatibilizers on Poly (lactic acid) (PLA) Properties after Extrusion Process. *Polymers* 2020, 12, 2688. https://doi.org/10.3390/polym12112688
35. Xuan, W.; Hakkarainen, M.; Odelius, K. Levulinic Acid as a Versatile Building Block for Plasticizer Design. *ACS Sustainable Chem. Eng.* 2019, https://doi.org/10.1021/acssuschemeng.9b02439
36. Mascia, L.; Kouparitsas, Y.; Nocita, D.; Bao, X. Antiplasticization of Polymer Materials: Structural Aspects and Effects on Mechanical and Diffusion-Controlled Properties. *Polymers* 2020, 12, 769. https://doi.org/10.3390/polym12040769
37. Ruiz, E.; Orozco, V.H.; Hoyos, L.M.; Giraldo, L.F. Study of Sonication Parameters on PLA Nanoparticles Preparation by Simple Emulsion-Evaporation Solvent Technique. *Eur. Polym. J.* 2022, 173, 111307, https://doi.org/10.1016/j.eurpolymj.2022.111307
38. Buoso, S.; Belletti, G.; Ragno, D.; Castelvetro, V.; Bertoldo, M. Rheological Response of Polylactic Acid Dispersions in Water with Xanthan Gum. *ACS Omega* 2022, 7, 12536–12548, https://doi.org/10.1021/acsomega.1c05382
39. Keresztes, J.; Csóka, L. Characterisation of the Surface Free Energy of the Recycled Cellulose Layer that Comprises the Middle Component of Corrugated Paperboards. *Coatings* 2023, 13, 259. https://doi.org/10.3390/coatings13020259
40. Baklan, D.; Bilousova, A.; Wesolowski, M. UV Resistance and Wetting of PLA Webs Obtained by Solution Blow Spinning. *Polymers* 2024, 16, 2428. https://doi.org/10.3390/polym16172428
41. Elsawy, M.A.; Kim, K.H.; Park, J.W.; Deep, A. Hydrolytic Degradation of Polylactic Acid (PLA) and Its Composites. *Renew. Sustain. Energy Rev.* 2017, 79, 1346–1352, https://doi.org/10.1016/j.rser.2017.05.143
42. Lee, S.; Wee, J.-W. Effect of Temperature and Relative Humidity on Hydrolytic Degradation of Additively Manufactured PLA: Characterization and Artificial Neural Network Modeling. *Polym. Degrad. Stab.* 2024, 230, 111055, https://doi.org/10.1016/j.polymdegradstab.2024.111055
43. Li, N.; Link, G.; Jelonnek, J. 3D Microwave Printing Temperature Control of Continuous Carbon Fiber Reinforced Composites. *Compos. Sci. Technol.* 2019, 187, 107939, https://doi.org/10.1016/j.compscitech.2019.107939
44. Asakura, T.; Ibe, Y.; Jono, T.; Naito, A. Structure and Dynamics of Biodegradable Polyurethane-Silk Fibroin Composite Materials in the Dry and Hydrated States Studied Using 13C Solid-State NMR Spectroscopy. *Polym. Degrad. Stab.* 2021, 190, 109645, https://doi.org/10.1016/j.polymdegradstab.2021.109645